

KERNFORSCHUNGSZENTRUM

KARLSRUHE

Oktober 1967

KFK 636
SM 101/10
EUR 3680 e

Institut für Reaktorentwicklung

Systems Analysis of a Fast Steam-Cooled Reactor of 1000 MWe

W. Frisch, F. Hofmann, E. Kiefhaber, H. Moers, K. Schramm
D. Smidt, H. Spilker



GESELLSCHAFT FÜR KERNFORSCHUNG M. B. H.

KARLSRUHE

Als Manuskript vervielfältigt

Für diesen Bericht behalten wir uns alle Rechte vor

Gesellschaft für Kernforschung m.b.H.

Karlsruhe

October 1967

KFK 636

SM 101/10

EUR 3680 e

Institut für Reaktorentwicklung

SYSTEMS ANALYSIS OF A FAST STEAM-COOLED REACTOR OF 1000 MW(e)^{ж)}

W.Frisch

F.Hofmann

E.Kiefhaber жж)

H.Moers жжж)

K.Schramm

D.Smidt

H.Spilker

Gesellschaft für Kernforschung mbH., Karlsruhe

ж) Work performed within the association in the field of fast reactors between the European Atomic Energy Community and Gesellschaft für Kernforschung mbH., Karlsruhe

жж) Institut für Neutronenphysik und Reaktortechnik

жжж) Delegated from Gutehoffnungshütte Sterkrade AG., Oberhausen

INTERNATIONAL ATOMIC ENERGY AGENCY
SYMPOSIUM ON FAST REACTOR PHYSICS
AND RELATED SAFETY PROBLEMS
October 30 - November 3, 1967
Kernforschungszentrum Karlsruhe, Germany

SM 101/10

SYSTEMS ANALYSIS OF A FAST STEAM-COOLED REACTOR OF 1000 MW(e)[⌘]

W.Frisch, F.Hofmann, E.Kiefhaber,
H.Moers, K.Schramm, D.Smidt, H.Spilker

(Presented by D.Smidt)

Summary

The Karlsruhe design of a steam cooled fast reactor (D1) has been subject of a systems analysis. Here the dependence of fuel inventory, breeding ratio, rating, core geometry and plant efficiency on coolant pressure, and coolant temperature has been studied for two different rod powers. The effect of artificial surface roughness has been investigated. For some configurations the resulting fuel cycle and capital costs have been determined and discussed.

The main influence results from pressure. The lower pressure allows for higher breeding ratios, but lower efficiencies and vice versa. From this the fuel cycle costs show an optimum in the range of 150 ata. The capital costs on the other side decrease with pressure. The overall optimum of the power generating costs for the presently studied parameter range is at about 170 ata, a coolant outlet temperature of 540°C and a rod power of 420 W/cm. Artificial roughness (boundary layer type) leads for a required system pressure and outlet temperature to a larger coolant volume fraction, and, therefore, to reduced breeding ratios, but higher efficiencies.

As another part of the work some stability characteristics of the cores have been studied. The dependence of the core stability on the varied parameters is shown.

⌘) Work performed within the association in the field of fast reactors between the European Atomic Energy Community and Gesellschaft für Kernforschung mbH., Karlsruhe

1. Introduction

The design of a steam cooled fast breeder reactor (D1) [1] was subject of a systems analysis. It comprises a systematic variation of various design parameters of the core and its influence on the power generating costs. One of the problems of this investigation was the lack of reference points from other designs, another one the great number of independent parameters, which had become evident already during the work on the D1 study. The broad field of possible variations had to be narrowed down to permit the target to be reached within a reasonable time. Thus, to mention just one important possibility of variation, the design concept, i.e. the external structure and the flowsheet of the plant, were incorporated from D1 without any change. On this basis the dynamic, safety and thermodynamic nuclear considerations are developed.

A major objective of the thermohydraulic, nuclear and cost investigations communicated in this report was the possibility of making qualitative statements about the economical potential of a steam-cooled breeder reactor and, in addition, to establish quantitative design criteria for a prototype. Here, the preference of low power generating costs or a high breeding ratio played a special part. Therefore in particular the coolant pressure was varied between 120 and 170 ata to show clearly to what extent the higher breeding ratio at lower pressures must be paid for in terms of reduced economy.

The dynamic and safety investigations for the D1 plant carried out at the same time are reported elsewhere [2]. Only the influence of the varied parameters on some interesting dynamic characteristics are dealt with.

2. Characteristic Data of the 1000 MW(e) Reference Reactor (D1 Study)

The nuclear reactor facility used as the basis for these studies is a steam cooled fast breeder reactor with two steam turbines of 500 MW(e) each in a direct cycle. One of the main features is the external generation of the saturated steam which is superheated in the reactor and taken to the consumers, i.e. secondary steam generator, reheater, injection evaporator, and the turbines (Fig.1).

The reactor steel vessel houses the cylindrical core which is surrounded by the blanket and the internal shield. The core itself consists of two zones of different fuel enrichment. It consists of 163 hexagonal fuel elements with 469 fuel rods each. Integral parts of the core elements are the upper and the lower axial blankets which, therefore, have to be exchanged together with the core elements, while the exchange cycle of the radial blanket elements can be determined independently upon economical view points.

To reduce the moderating effect of the coolant to a minimum, the coolant fraction has to be small. 32 vol. % were chosen as a practical minimum.

The coolant enters the reactor at the bottom, flows first upward through the radial blanket and then downward through the core and the axial blankets into the inner one of two concentric tubes at the bottom of the reactor vessel. The steam conditions at the reactor outlet are 170 ata and 540°C. The net efficiency of the power plant was calculated to be 39.7 %.

Under the conditions outlined an overall breeding ratio of 1.15 was determined with a smeared fuel density of 87 % of the theoretical density. With an average burnup of 55.000 MWd/t of the fuel as discharged and a Pu price of \$ 10/g and a load factor of 0.7 a value of mills 1.3/kWh was calculated for the fuel cycle costs and mills 5.25/kWh for the power generating costs.

A detailed description of the reactor plant is given in the reference design study of the steam cooled fast breeder reactor [1].

3. Parameters

3.1 Independent Parameters

The main objective of the analysis consisted in investigating the influence of the most significant design parameters upon the costs of power production. These main parameters were varied within reasonable limits, corresponding to the special requirements of steam cooling:

- a) The system pressure p_2 was varied from 120 to 170 ata at reactor outlet. The lower limit is due to the fact that, in analogy to D1, reheating is planned. At pressures above 170 ata the breeding gain will decrease drastically.
- b) The coolant temperature ϑ_2 at the reactor outlet was another parameter which was varied between 480°C and 560°C. The lower limit is dictated by the required steam quality at the end of expansion, the upper one by the properties of the materials chosen for the turbine.
- c) The max. nominal linear rod power χ was varied within the limits of 370 - 420 W/cm.

Compared to the D1 study it was possible to increase the rod power in general on the basis of an improved analysis of the hot channel factors. The values of χ apply to the maximum linear rod power without hot channel factors. Considering these factors and burnup increases the values by some 15 %.

In another investigation the influence of turbulence promoters was analysed.

As a consequence of the variations mentioned above, the following properties were varied:

Core geometry, net efficiency, critical mass, breeding ratio of the individual zones, specific power and hence necessarily, capital and fuel cycle costs.

3.2 Parameters Kept Constant

The following parameters are taken directly from the D1 study ($Q_{e1} = 1000 \text{ MW}(e)$) without variation:

- a) The maximum can temperature T_{max} in the hot channel (hot channel factor included) is not to exceed 700°C because of creep collapse. This value will be encountered at the hot spot on the inside of the fuel can, considering cross mixing of the coolant as it is possible with the helical spacers. Because of the poorer heat transfer properties with steam as compared to sodium (a factor of about 10) the temperature of the can, in addition to the temperature in the center of the fuel, became a special criterion of core design.

- b) The diameter of a fuel rod with can is 7 mm; the thickness of the wall of the can is 0,37 mm.
- c) Apart from the investigations with turbulence promoters the volume fraction of the coolant α in the core and in the axial blanket was restricted to the minimum of 32 vol. % in the interest of a good breeding ratio; this value is the minimum permissible from the engineering standpoint.
- d) For the other core materials the volume fractions are as follows:
- | | |
|-------------------------------------------------------|-------------|
| Structural material in the core and the axial blanket | 20.6 vol. % |
| Fuel (oxide fuel) in the core | 45.4 vol. % |
| in the radial blanket | 55.6 vol. % |
| Control rod follower (Al_2O_3) | 2.0 vol. % |
- e) The canning and structural materials are:
- | | |
|-----------------------------------|--------------|
| In the core and the axial blanket | Inconel 625 |
| In the radial blanket | Incoloy 800. |
- f) The nuclear calculations are carried out with the ABN 26 group constants set.
- g) The smeared density of the fuel is 87 % of the theoretical density; the isotopic Pu composition is 74/22.7/2.3/1.0.
- h) The average burnup over time is 27.500 Mwd/t.
- i) The volumes of the two core areas of different enrichments always are of equal size.
- k) The enrichment in the two core areas is selected such as to make the maximum power densities in the two zones equal and cause the reactor to reach the desired criticality.
- l) For the reactors investigated an axial and radial blanket thickness of 35 cm is assumed.
- m) The evaluation of the fuel cycle costs is based on a plant lifetime of 25 years at 70 % load factor. In the calculations fuel transport costs of \$ 5/kg and delays of 0.5 years in fabrication and 0.6 years in reprocessing were taken into account.
- n) For the capital investment an interest rate of 7 % and a tax rate of 2.7 % as well as a 1 % insurance rate are assumed.
- o) The price of the plutonium and the depleted uranium is included in the calculations with rates of \$ 10/g and \$ 3/kg, respectively.

4. Methods of Calculation

4.1 Flowsheet

The flowsheet is shown in Fig.2 . On the basis of estimated values of net efficiency, rod power, power distribution and can temperature the thermodynamic calculation first determines the core configuration,

pressure losses in the reactor and the temperature distribution in the core in the first approximation. The following calculations of reactor physics and hot channel factors together with the results of the calculations for the coolant circuits result in new values of net efficiency, rod power, axial power peak factor and maximum can temperature. In this way the required design quantities net electrical power, max. linear nominal rod power and maximum can temperature were determined by iteration. Finally the power generating costs are evaluated.

4.2 Thermodynamic Cycle Calculation

The thermodynamic calculation of the circuits is performed by means of a digital program [3]. On the basis of the input data, such as net electrical power, steam pressure and temperature at reactor outlet, and pressure drop in the reactor, this program calculates mass flows, steam conditions, and net efficiency for the whole cooling circuits including all energy losses. The design analysis of the components of the circuits (steam generator, reheater, blower) is then carried out, also by digital programs [4,5], on the basis of the mass flows and steam conditions determined.

4.3 Thermodynamic Reactor Model

The model of the thermal calculation of the reactor starts with the assumption of a cosine shaped power distribution in the axial direction in the core. It accounts for the better heat transfer in the bundle compared with the circular tube. The calculation of the core is performed in several axial zones in each case with and without turbulence promoters. The corresponding changes in the state variables and properties of the steam are included in the calculation as functions of pressure and temperature.

4.4 Nuclear Calculations

For the core configuration given by thermodynamics the interesting nuclear quantities, i.e. critical mass, breeding ratio of the individual zones and the power peak factors, are calculated with the Karlsruhe nuclear program system NUSYS. Suitable use of results of zero and one dimensional calculations permit a considerable reduction in computing time required for the two dimensional calculations.

4.5 Cost Calculations

As was mentioned above, the D1 study supplied the plant concept and the flowsheet of the circuit for the systems analysis. The varied reactor parameters by necessity resulted in changes or rather adaptations also of the rest of the cycle. A digital program was used to evaluate the necessary design changes. The influence of these design modifications upon direct plant costs were taken into account. Also the influence of changes in core geometry upon the costs of pressure vessel, containment and reactor building are included in the analysis. Plant components and reactor systems which do not specifically depend on steam conditions were included under the prices corresponding to the D1 data.

The fuel cycle costs are calculated by using the digital program BAKO [6]. The input data required are taken from two dimensional nuclear calculations. These are the geometry of the zones, their fuel and fertile material compositions, and the corresponding breeding ratios.

Moreover, other input data are the thermal power, net efficiency and burnup. The program then calculates, for various thicknesses of the axial and radial blankets and different lifetimes of the radial blanket, in addition to the detailed costs the specific fuel cycle costs. In case the direct and indirect capital costs are fed in, also the specific capital and energy generating costs are computed.

The most important cost terms of fuel cycle cost are the costs of fuel element fabrication, reprocessing, and of fissile material. For a given fuel fabrication plant throughput the fabricating costs are calculated for the core elements by the formula

$$(1) \quad K_{FC} = 86.1 + 4100 \left(\frac{1}{DPIN} + \frac{0.62}{DPIN^2} \right) \left(1 - \frac{HC}{278} \right) \quad [DM/kg]$$

In this formula $DPIN =$ diameter of the pellets [mm] and $HC =$ height of core [cm]. At constant pin diameter this results in core fabricating costs which are dependent only on the core height.

5. Results

5.1 Thermodynamic and Nuclear Results

The most important results of the thermodynamic and nuclear investigations will be discussed on the basis of Fig. 3 - 6. The figures show the influence of system pressure, coolant outlet temperature, and rod power on the net efficiency of the plant η_N and on core geometry (core volume V_c , ratio of core height/core diameter H_c/D_c) and on the breeding ratio BR, critical mass M_{crit} , and rating RA.

5.1.1 Influence on Net Efficiency

The net efficiency (Fig.3) rises with increasing system pressure, mainly due to the increasing density and specific heat capacity (less pumping power) of the steam. The step from 120 to 150 ata contributes about twice as much gain (about 3 percent absolute) as the transition from 150 to 170 ata.

An increase in the coolant outlet temperature, on one hand, results in an increase in the thermodynamic efficiency, however, on the other hand, under the boundary conditions postulated ($T_{max} = \text{const.}$, $\alpha = \text{const.}$) it also requires an increase in pumping power for the reactor. The resulting net efficiency, therefore, increases as a function of coolant outlet temperature only as long as the gain in thermal efficiency exceeds the corresponding losses due to increased pumping power. Fig. 3 illustrates that the net efficiency will gradually rise with temperature to the peak and then drop very rapidly. The peaks move towards higher coolant outlet temperatures with increasing system pressure, namely from 120 ata to 170 ata while going from $t_2 \approx 500^\circ\text{C}$ to $\approx 540^\circ\text{C}$.

Because of the higher pumping power in the core (larger coolant mass flow and core height^{*)}) an increase in rod power is at the expense of the net efficiency.

*) see section 5.1.2

5.1.2 Influence on Core Geometry

As has been said earlier, the net efficiency of the plant increases with rising system pressure. This means that the gross power to be generated in the core and hence also the core volume will become smaller with increasing system pressure (Fig.4a). Under the boundary conditions listed in section 3.2, in particular the fact that the can temperature should not exceed 700°C, the investigations also show the core height to change but little with rising system pressure. (In a change from 120 to 170 ata there is some 3 - 4 % change in core height). This has only a minor feedback upon the axial power peak factor. The volume change as a function of system pressure, therefore, is caused essentially by the change in the core diameter ($V_c \sim D_c^2$). The ratio of core height/core diameter changes only little in the process (Fig.4b, 5b).

However, under the existing boundary conditions ($T_{\max} = \text{const.}$, $\alpha = \text{const.}$) an increase in the coolant outlet temperature requires a considerably stronger increase in the core height. In a transition from 500°C to 540°C the core height increases by about 50 %. This results in higher pressure loss and also a worse axial power peak factor. On the whole, a higher outlet temperature causes a greater core volume and at the same time a considerable increase in the ratio of core height/core diameter (Fig.4a, 4b).

Because of the higher power density an increase in rod power will result in a roughly proportional reduction of the core volume and a roughly proportional increase in the coolant velocity (Fig.5a). In order to be able again to keep within the required can temperature, the core height is bound to increase slightly at a given core outlet temperature so that the ratio H_c/D_c becomes larger also in this case (Fig.5b).

5.1.3 Influence on the Breeding Ratio and the Critical Mass of Fissile Material in the Core

The dependence of the breeding ratio and the critical fuel mass in the core on pressure (Fig.6a, 6b) can be understood more easily if one considers that with rising pressure the neutron spectrum will become softer because of the higher coolant density. This decreases the average η -value of the fuel (worse η -value of plutonium and less fast fission; $\eta = \frac{\nu \Sigma_f}{\Sigma_a}$) so that the enrichment has to be increased, which results in a reduction of the breeding ratio. An additional reduction of the breeding ratio is caused by the fact that the capture cross section of the fertile material below an average neutron energy of 100 - 200 keV increases less markedly towards lower energies than the absorption cross section of the fissile material. On the other hand, there is a reduction in the critical mass with rising pressure (up to 10 %), because the increase in enrichment with rising pressure is more than compensated, by the simultaneous reduction in the core volume.

The changes in geometry required in the case of an increase in the coolant outlet temperature result in a reduction of the geometrical buckling B^2 . This leads to somewhat less external breeding, which has a negative influence upon the total breeding ratio. The changes in geometry mentioned above, are of such a kind, however, as to make the height increase sharply and the diameter decrease markedly. This

shifts the external breeding process from the axial into the radial blanket, which has a favourable influence upon the breeding ratio in the D1 reactor (caused by the higher fuel volume fraction in the radial blanket and the use of Incoloy 800 instead of Inconel 625). This effect is much more marked than the effects of a reduction of B^2 so that, on the whole, there is a definitive increase in the overall breeding ratio (about 0.03 - 0.04) with rising outlet temperature. Upon the critical mass of fuel an increase in the coolant outlet temperature has two opposite effects:

- a) the core volume increases, as explained under 5.1.2,
- b) the enrichment decreases because of the smaller leakage losses (reduction of B^2).

These two effects almost compensate, except for slight differences which depend on the pressure and the rod power.

With the increase in rod power the change in core diameter is considerably smaller than with the previously discussed increase in coolant outlet temperature. The breeding process, which is more favourable in the radial blanket, thus can have only a weak effect so that also the increase in the breeding ratio is much smaller than in the case of increasing the outlet temperature. The volume reduction connected with the increase in rod power almost completely results in a reduction of the critical mass of fissile material in the core due to the nearly unchanged enrichment.

5.1.4 Influence Upon Rating

In accordance with the usual definition the rating was calculated as

$$RA = \frac{Q_{th}}{M_{crit}} = \frac{Q_{el}}{\eta_N \cdot M_{crit}}$$

It changes only very slightly at constant electric power as a function of the system pressure and the coolant outlet temperature because of the controversial behaviour of net efficiency η_N and critical mass M_{crit} (a maximum change of 1.5 % (Fig.6c)). As a function of rod power, however, the change is very marked (≈ 12 %), especially so because of the big change in critical mass.

5.2 Results of Cost Calculations

Fig.7 represents the capital cost trends of four important groups of components of the plant. The "reactor" group (Fig.7a) comprises the core support components, e.g. core support plate, upper core guide plate, core clamping and other reactor internals and the pressure vessel itself with top shield, superheated steam and saturated steam headers with studs. The entries under "reactor building" (Fig.7b) include the costs of foundation of the reactor building, all the concrete installations, the steel containment and the outer concrete shell. Fig.7c summarizes the costs of the plant components under the heading of "cooling circuits" as there are various circulation blowers, injection steam generators, secondary steam generators, steam accumulator, feed pumps and the corresponding piping. The "turbine system" shown in Fig. 7d includes the two turbo machines with condensers, reheaters and the interconnecting pipes.

The partially strong degression and, respectively, progression of the costs shown in these figures for the various groups of components appears less pronounced when the costs of these components are added which do not specifically depend on changes in the steam parameters.

The overall direct capital cost trend of the investigated plants is shown in Fig.8. This figure shows that the direct plant costs for the same reactor outlet temperature and rod power change only 3.3 % in the transition from 120 to 170 ata at the maximum.

The indirect capital costs are taken generally as 30 % of the direct costs. They include contingencies, engineering expenses of the customer and start up costs.

The fabrication costs of the core fuel elements depend, as already mentioned in our cases only on the core height. According to equation (1) in chapter 4.5 this results in decreasing fabricating costs per kg with rising outlet temperature. The weighting of these costs including the costs of the axial and radial blankets with the corresponding amounts of fuel results in less expenditure for the high rod power. After distribution over the generated power the curves shown in Fig.9a then exhibit a plot proportional to $1/\eta_N$

The decreasing trend of the reprocessing costs with rising pressure in Fig. 9b is due to the change in fuel masses. The cost differences at constant pressure but varied outlet temperature and rod power are due to the differences in efficiency.

In the costs of fissile material plotted in Fig.9c the influences of various parameters superimpose. Rising pressure, on one hand, increases net efficiency, i.e. decreasing costs and, on the other hand, a lower breeding ratio, that implies rising costs, which explains the occurrence of a minimum in the curves. Higher rod power at constant temperature results in an improved breeding ratio and a lower net efficiency; both have an influence on costs in a way that the minimum hardly shifts with pressure. At constant rod power and rising outlet temperature the increasing net efficiency and the improved breeding ratio also have a cost decreasing effect, but the minimum shifts toward higher pressures with higher temperature due to the more marked change in the breeding ratio.

The costs of the fissile material also include interest rates and the reimbursement for the bred plutonium. While the first factor results in cost savings with rising pressure because of the smaller amounts of fuel, the plutonium reimbursement term results in increasing costs with higher pressure because of the proportionality with $(\frac{BR-1}{\eta_N})$, since both BR and η_N are influenced in an unfavourable way.

The total fuel cycle costs are shown in Fig.10, which also includes the costs of fuel transport. The total fuel cycle costs dealt with in the figure and table I are calculated for a lifetime of the radial blanket at about two core times.

Summing up the specific fuel cycle and capital costs results in the total cost of power generating plus a constant amount for plant operating cost (mills 0.3/kWh)(Fig.11). The plot shows the cost minimum to shift towards higher pressures with rising temperatures. The maximum cost gain arising out of a transition from 120 to 170 ata appears

with the highest rod power and coolant temperature. The cost decreases in this case from mills 4.2/kWh to mills 4.05/kWh.

The cost program also allows the determination of the doubling times for the different reactors. They are shown in Fig.12. The analysis has made evident, that the most favourable reactors from the viewpoint of doubling time are the reactors with the highest power generating costs

5.3 Influence of Turbulence Promoters

For a system pressure of 120 ata at core outlet the influence of an artificial roughening [7] was investigated and compared to a case of a smooth surface with respect to possible improvement of heat transfer. This roughening consists of circumferential transverse fins with rectangular cross section over only 75 % of the core height so as to keep the necessary increase in compressor power as a consequence of the roughening effect as low as possible. With respect to the producibility and the arising corrosion phenomena the values of the following ratios were fixed:

$$\frac{\text{fin pitch}}{\text{fin height}} = 10$$

$$\frac{\text{fin height}}{\text{equiv.diameter}} = 0.015$$

This type of surface roughening increases the local heat transfer coefficient by about a factor of three and the friction factor by about a factor of nine.

The results shown in Fig.13 are the net efficiency and the ratio H_c/D_c as functions of the coolant outlet temperature for smooth fuel elements and for elements equipped with turbulence promoters. The coolant fraction α is 32 vol.%, the rod power $\chi = 420$ W/cm, the maximum can temperature $T_{\max} = 700^\circ\text{C}$ in both cases.

It is shown that roughening will generally improve the efficiency, with the relative maximum shifting towards higher outlet temperatures. With respect to the core geometry this requires a marked flattening of the cores. For the case represented here the maximum efficiency increases from ≈ 36 % at 500°C (smooth case) to ≈ 37 % at 540°C (rough case). The H_c/D_c ratio drops by about 50 % (from 0.3 to 0.15).

However, if the same core geometry as in the smooth case is to be maintained, it is necessary with constant coolant volume fraction (Fig.13) to increase the outlet temperature considerably. For H_c/D_c ratios larger than 0.3 the outlet temperature assumes values already exceeding 580°C . At outlet temperature as high as this, there will no longer be any gain in terms of efficiency, let alone the problems of turbine materials.

Fig.14 shows the influence of the coolant fraction α on the roughening described above. The same conditions apply as in Fig.13. It is seen that an increase in the coolant fraction results in an additional increase in efficiency. The relative peaks shift towards an even higher outlet temperature (cf. Fig.13). In the transition from $\alpha = 32$ vol.% to 50 vol.% the peak changes from $\approx 540^\circ\text{C}$ to $\approx 580^\circ\text{C}$, the efficiency rising by 1 - 2 % absolute.

With respect to the core geometry an increase in α at constant outlet temperature results in an increase in the H_c/D_c ratio. However, in order to obtain values for H_c/D_c of ≈ 0.3 to 0.6 in a reasonable temperature range $\vartheta_2 \approx 560^\circ\text{C}$ it is necessary to increase the coolant fraction to more than 45 vol.%. This has a very negative effect on the total breeding ratio. Moreover, the gain in terms of efficiency will be less.

Another possibility of increasing the H_c/D_c ratio is reducing the maximum can temperature at constant outlet temperature (Fig.15: rough case; $\alpha = 37$ vol.%; $\chi = 420$ W/cm). However, this always entails a loss in efficiency which very strongly increases with rising outlet temperature. Also at constant H_c/D_c the transition to a lower can temperature results in a reduction in efficiency. The desirable tendencies, lower can temperature ($T_{\max} < 700^\circ\text{C}$), lower outlet temperature ($\vartheta_2 < 560^\circ\text{C}$) and larger H_c/D_c ($H_c/D_c > 0.3$) thus have to be paid for by a smaller efficiency in any case.

Finally it should be pointed out here that the results of artificial roughening discussed in this section apply to a power of 1000 MW(e). For smaller reactors it is still possible that artificial roughening would improve the core performance more significantly.

5.4 Core Stability

The main investigations of the dynamics and the safety of the D1-plant are represented in a special report [27]. The influence of varied parameters on the power coefficient and the distance from the stability boundary is represented here. Both quantities are a characteristic for stability and safety.

The power coefficient $\frac{\Delta k}{\Delta P/P}$ is a measure for the feedback reactivity induced by a power change. The stability condition for the core is

$$\frac{\Delta k}{\Delta P/P} < 0.$$

The relative distance from the stability boundary $\frac{\alpha_\vartheta}{\alpha_{\vartheta_{gr}}}$ is a stability characteristic related to the important coolant density coefficient α_ϑ . $\alpha_{\vartheta_{gr}}$ is the coolant density coefficient at the stability boundary,

α_ϑ the value achieved from the nuclear calculations.

The stability condition is $\frac{\alpha_\vartheta}{\alpha_{\vartheta_{gr}}} < 1$.

Fig.16 shows $-\frac{\Delta k}{\Delta P/P}$ and $\frac{\alpha_\vartheta}{\alpha_{\vartheta_{gr}}}$ as functions of p_2 , χ and ϑ_2 for a mean burnup. Increase of the rod power χ and decrease of the outlet temperature ϑ_2 lead to an improvement in stability. With increasing system pressure stability becomes better, especially at $\vartheta_2 = 500^\circ\text{C}$.

6. Conclusions

- a) The maximum of the net efficiency sharply depends on system pressure and coolant outlet temperature. Increasing rod power leads to a lower efficiency.
- b) Increasing pressure allows for a smaller core volume at nearly unchanged core height. Higher rod power allows for lower core volumes.
- c) The breeding ratio decreases with increasing pressure and decreasing coolant temperature. Higher rod powers lead to higher breeding ratios. The critical mass decreases with increasing pressure and is decreased with increasing rod power.

- d) The rating nearly is unchanged with system pressure and coolant outlet temperature.
- e) The fuel cycle costs show an optimum which mainly depends on pressure and temperature. At 500°C reactor outlet temperature it is in the range of 150 to 160 ata. It shifts to higher pressures with increasing temperature at lower costs. An increase in rod power decreases costs but does not change the mentioned tendency.
- f) The direct capital costs decrease with increasing pressure. The rod power has a negligible influence on capital costs.
- g) The power generating costs sharply depend on system pressure in the range of 120 to 150 ata. At higher pressures the main influence is given by temperature and rod power. The lowest power generating costs appear at high pressure, high temperature and high rod power.
- h) Artificial roughness means an increase in net efficiency, and for 1000 MW(e) a strong flattening of the cores. It can be compensated by
 - 1) an increase of the coolant volume fraction, i.e. lower total breeding ratio,
 - 2) an increase of the coolant outlet temperature, i.e. problems with turbine materials,
 - 3) a decrease of the maximum can temperature, i.e. a lower net efficiency.

At a net electrical power less than 1000 MW(e) the same artificial roughening causes a lower flattening of the core. This leads to a smaller coolant volume fraction or a lower coolant outlet temperature for a constant H_c/D_c ratio.

- i) Higher rod power, higher system pressure and lower coolant outlet temperature lead to an improvement in stability.

Nomenclature

B^2	$[cm^{-2}]$	Geometrical buckling
BR		Total breeding ratio
H_c/D_c		Ratio: Core height/core diameter
K_{FC}	$[Dpf/kWh]$	Fuel cycle costs
M_{crit}	$[kg]$	Critical mass of fissile material
p_2	$[ata]$	System pressure at core outlet
Q_{el}	$[MW]$	Net electrical output
RA	$[\frac{MW(th)}{kg}]$	Rating
T_{max}	$[^{\circ}C]$	Maximum can temperature
V_c	$[m^3]$	Core volume
α		Coolant volume fraction
α_s	$[\frac{1}{g/cm^3}]$	Coolant density coefficient
$\frac{\Delta k}{\Delta P/P}$	$[\%]$	Power coefficient
η		Average number of neutrons produced per neutron absorbed
η_N		Net efficiency
ϑ_2	$[^{\circ}C]$	Coolant temperature at core outlet
ν		Average number of neutrons per fission
Σ_a	$[cm^{-1}]$	Macroscopic absorption cross section
Σ_f	$[cm^{-1}]$	Macroscopic fission cross section
χ	$[W/cm]$	Maximum linear rod power

References

- / 1 / Müller A., et al.: Referenzstudie für den 1000 MW(e) dampfgekühlten Schnellen Brutreaktor (D1). KFK 392 (1966)
- / 2 / Frisch W., et al.: Safety Aspects of Steam Cooled Fast Breeder Reactors. KFK 613 (1967)
- / 3 / Spilker H.: Ein Programm zur elektronischen Berechnung des thermodynamischen Kreisprozesses und des Kühlkreislaufes dampfgekühlter Kernreaktoren. KFK, Externer Bericht No. 8/66-2 (1966)
- / 4 / Schnauder H.: Rechenprogramm zur Auslegung von dampfbeheizten Zwischenüberhitzern. KFK, Externer Bericht No.8/66-3 (1966)
- / 5 / Schnauder H.: Rechenprogramm zur Auslegung von dampfbeheizten Dampferzeugern. KFK, Externer Bericht No. 8/66-4 (1966)
- / 6 / Jansen D.: BAKO - Ein Programm zur Kosten- und Strategienberechnung von Brüterkraftwerken mit der Barwertmethode. KFK 644 (1967)
- / 7 / Wilkie D.: Forced Convection Heat Transfer from Surfaces Roughened by Transverse Ribs. EAES-Heat Transfer Symposium on Superheated Steam or Gas (1966)

Varied Parameters

System Pressure	[ata]	120	120	120	120	150	150	150	150	170	170	170	170
Max. nom. Rod Power	[W/cm]	370	420	370	420	370	420	370	420	370	420	370	420
Core Outlet Temperat.	[°C]	540	540	500	500	540	540	500	500	540	540	500	500

Thermodyn.+ Nuclear Results

Core Diameter	[cm]	263	249	318	296	248	232	306	286	245	228	309	286
Core Height	[cm]	144	146	92	96	148	152	92	94	148	152	88	92
Net Efficiency	[°/o]	36.5	35.2	36.4	35.6	39.7	39.2	39.3	38.9	40.6	40.3	39.9	39.8
Core Pressure Drop	[at]	10.5	14.4	4.5	6.7	8.4	11.6	3.4	4.6	7.2	9.8	2.5	3.5
Coolant Mass Flow	[t/s]	4.01	4.17	4.68	4.81	3.54	3.61	4.23	4.28	3.38	3.44	4.06	4.09
Total Breeding Ratio		1.194	1.198	1.166	1.173	1.166	1.173	1.131	1.141	1.142	1.15	1.103	1.11
Mass of Fissile Mat.	[kg]	3236	2964	3226	2921	2996	2711	3029	2705	2945	2640	3030	2701
Mass of Fertile Mat.	[t]	25.7	23.4	23.8	21.6	23.5	21.1	22.0	19.7	23.1	20.5	21.6	19.4
Rating	[MW(th)/kg]	0.80	0.91	0.81	0.91	0.80	0.89	0.80	0.90	0.79	0.89	0.79	0.88

Costs Results

Direct Plant Costs	[10 ⁶ DM]	379.2	383.4	370.1	372.5	369.9	373.3	360.8	361.7	369.2	370.4	363.1	362.3
Fuel Cycle Costs	[Dpf/kWh]	0.526	0.515	0.578	0.554	0.496	0.474	0.552	0.525	0.493	0.469	0.56	0.531
Energy Gen.Costs	[Dpf/kWh]	1.7	1.7	1.72	1.71	1.64	1.63	1.67	1.65	1.63	1.61	1.68	1.65
Doubling Time	[a]	42.5	37	52	43.5	51	43.5	71	57	60.5	51	103	81.5

Stability

Power Coefficient	[β]	- 1.59	- 1.71	- 1.61	- 1.70	- 1.56	- 1.77	- 1.75	- 1.87	- 1.64	- 1.81	- 1.98	- 2.08
Distance from Stability Boundary		0.414	0.385	0.371	0.354	0.461	0.404	0.366	0.345	0.461	0.418	0.314	0.307

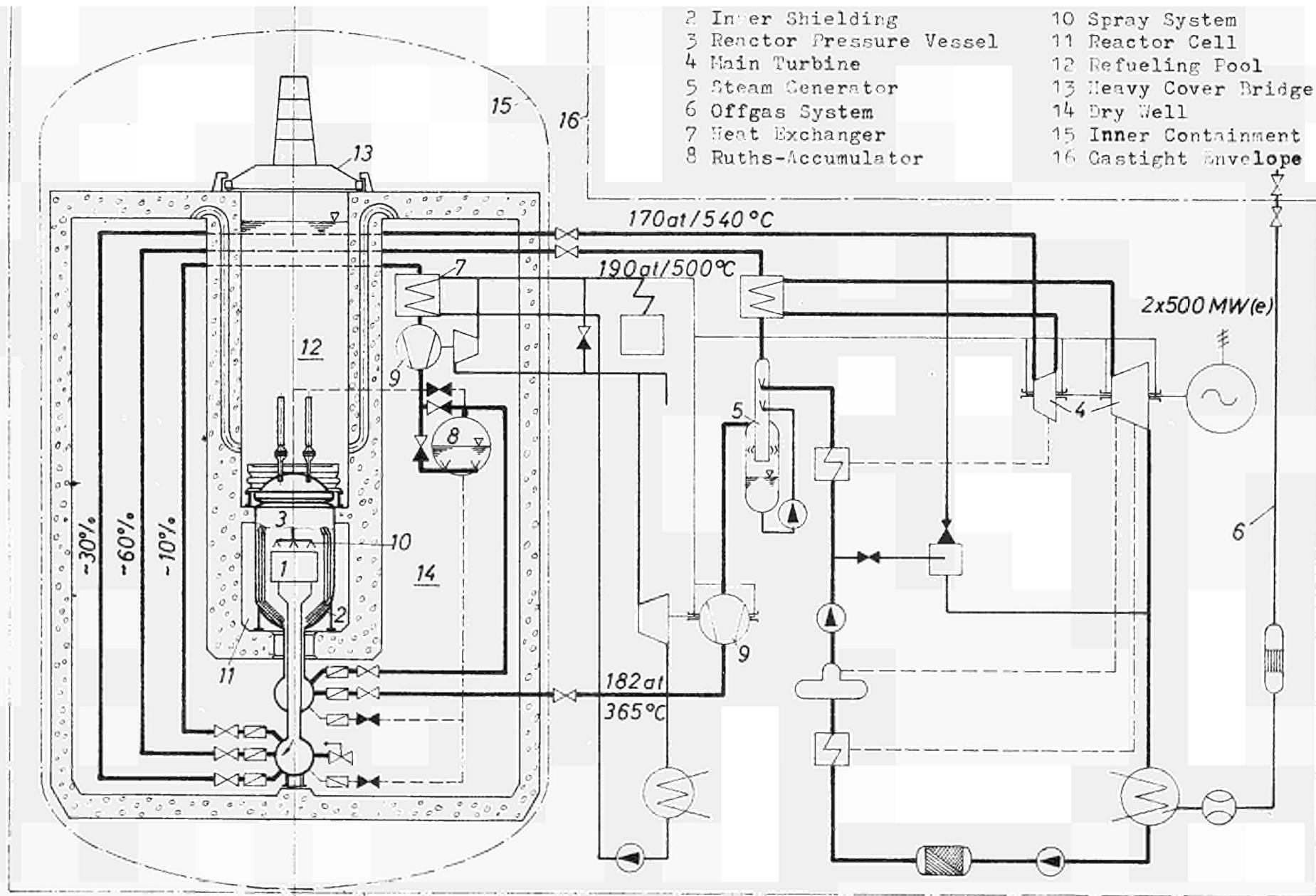


Fig. 1 Simplified Flow Diagram of the D1 Plant

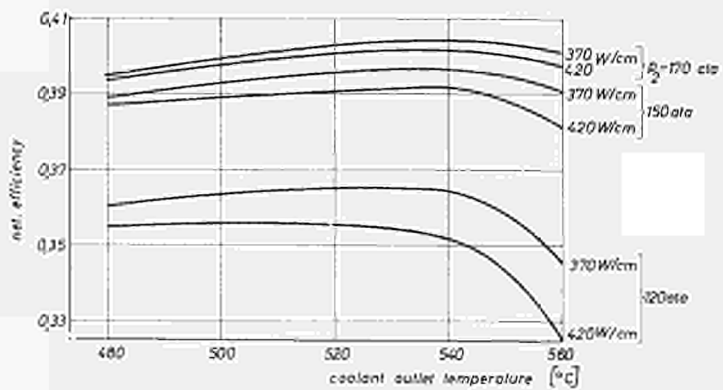


Fig.3 Influence of System Pressure and max. Rod Power

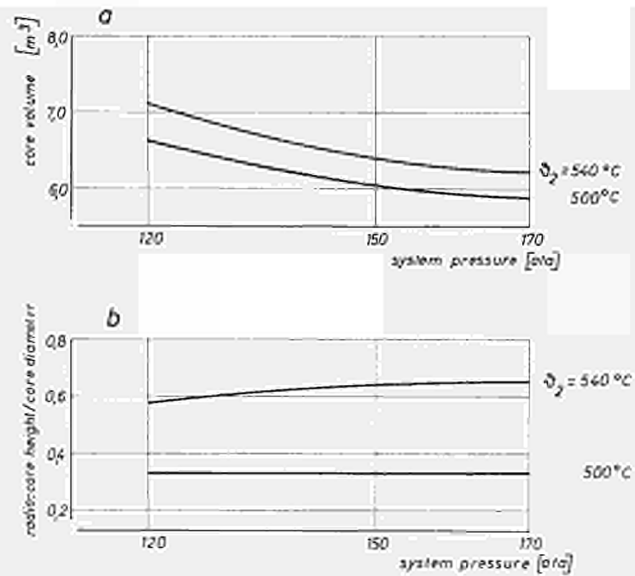


Fig.4 Influence of Coolant Outlet Temperature

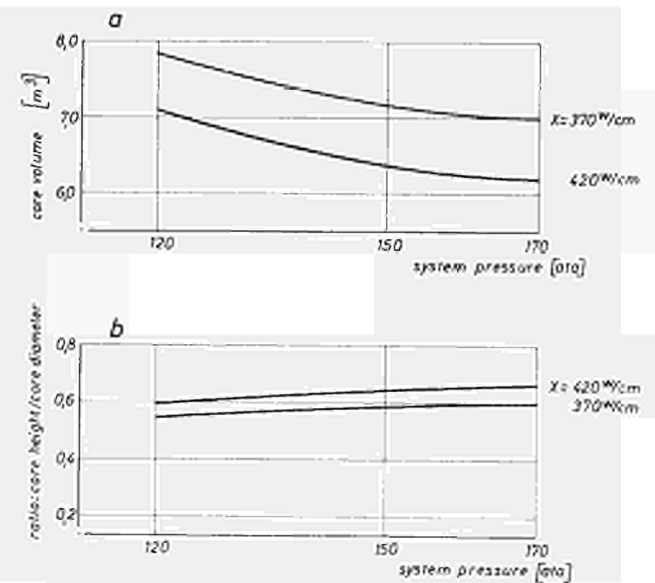


Fig.5 Influence of max. Rod. Power

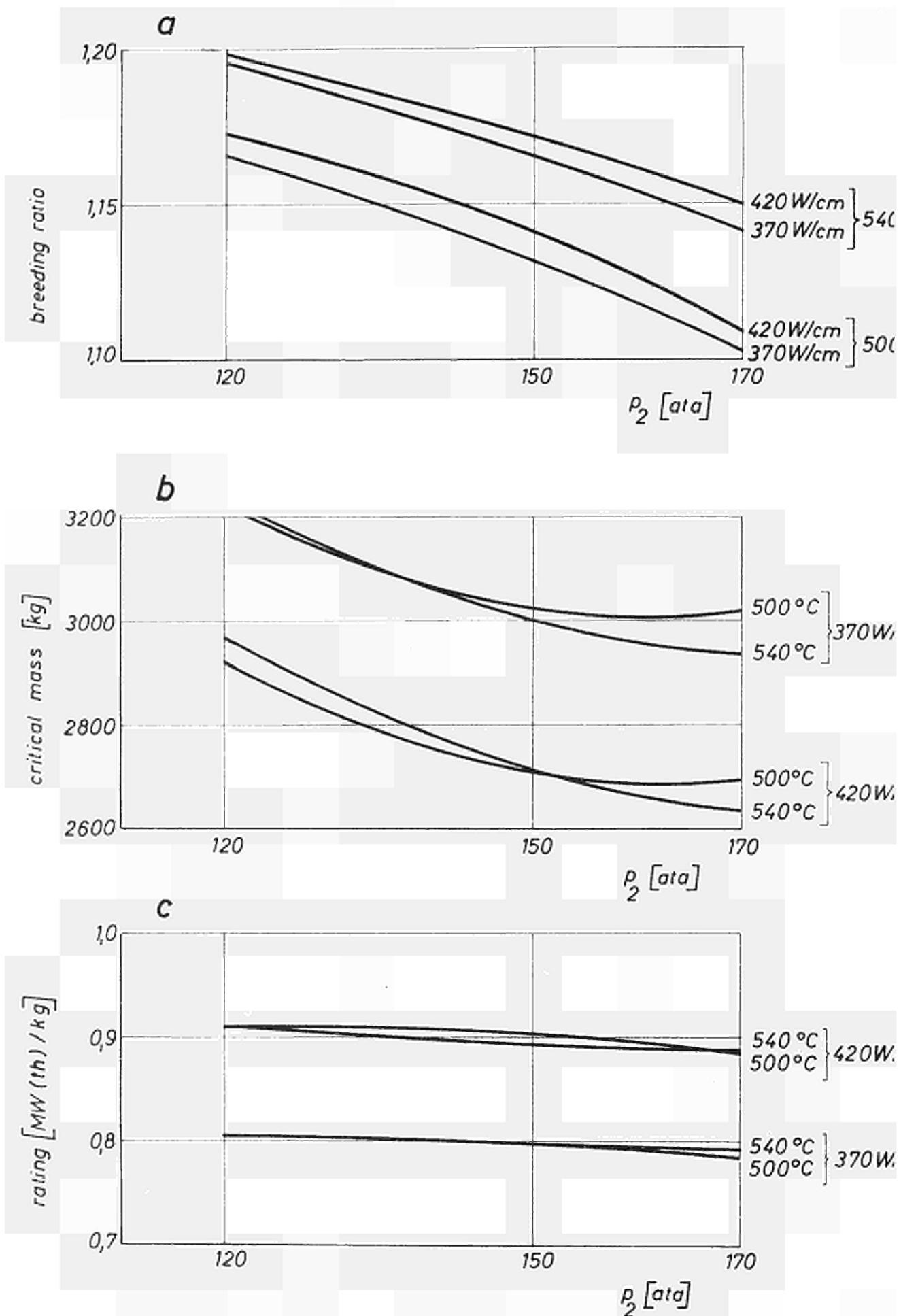


Fig.6 Influence of Coolant Outlet Temperature and max. Rod. Power

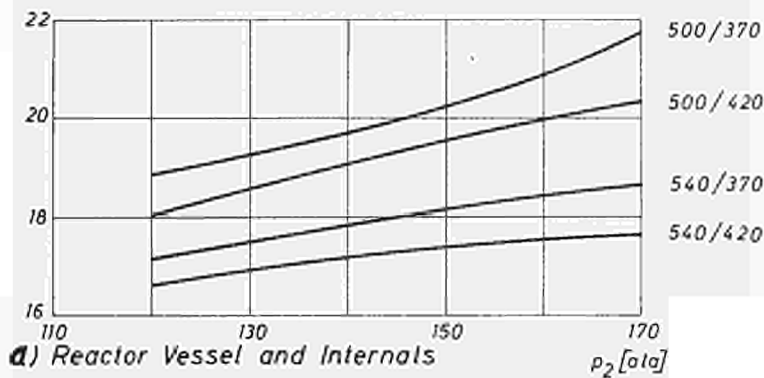
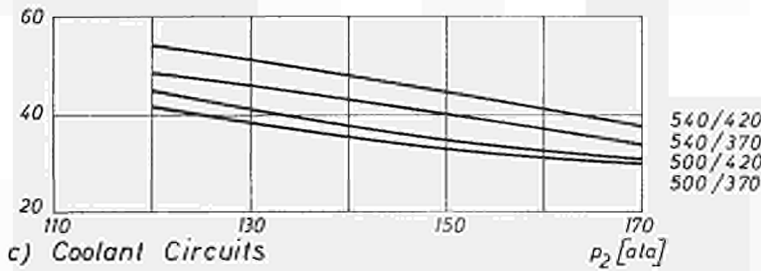
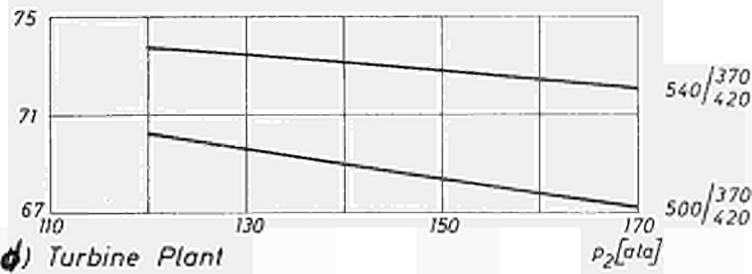
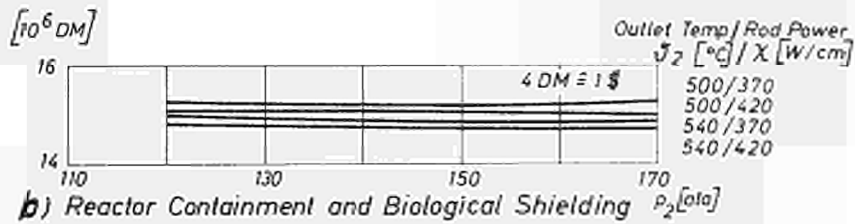


Fig.7 Different Components of Direct Plant Costs vs System Pressure

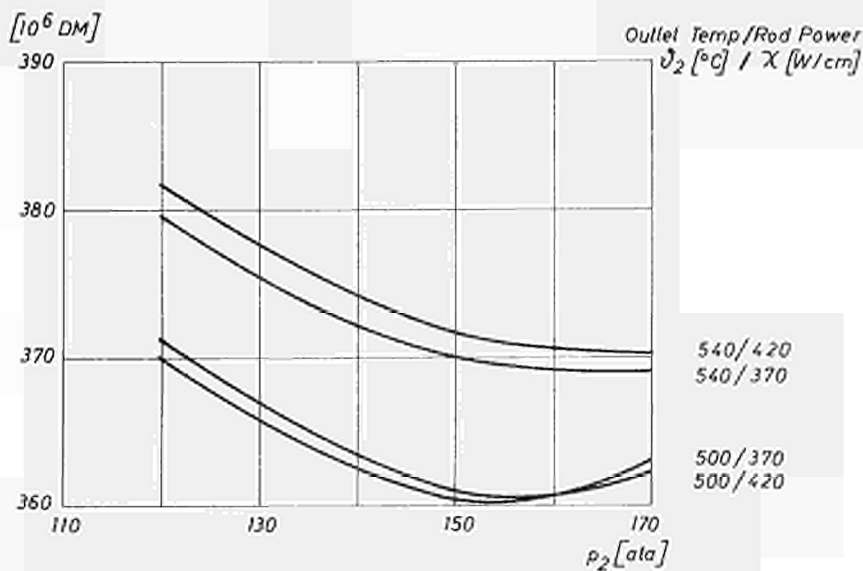
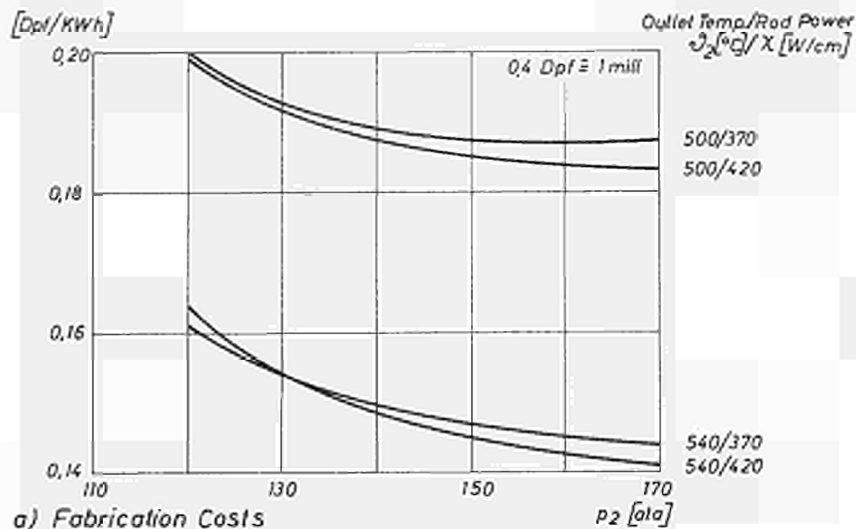
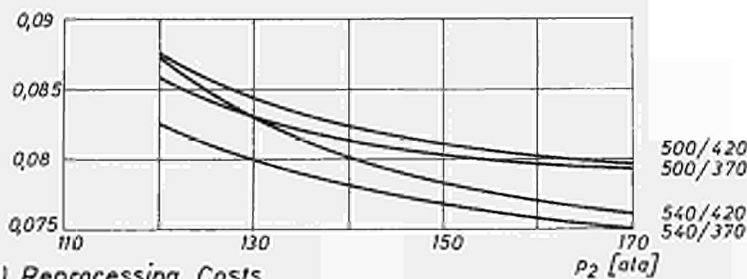


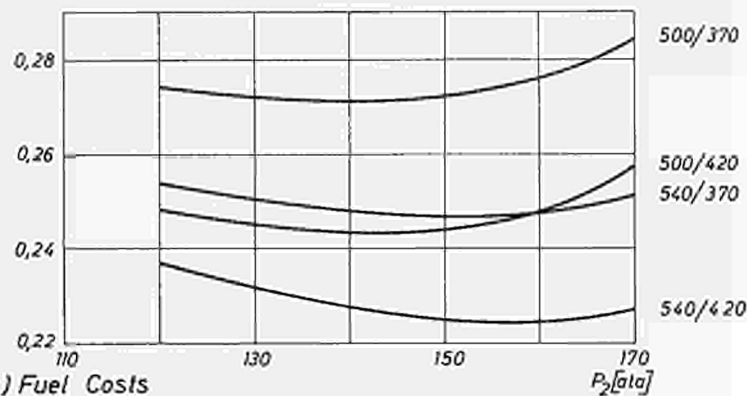
Fig.8 Direct Plant Costs vs System Pressure with ϑ_2 and χ as Parameters



a) Fabrication Costs



b) Reprocessing Costs



c) Fuel Costs

Fig.9 Different Parts of Fuel Cycle Cost vs System Pressure with X and T_2 as Parameters

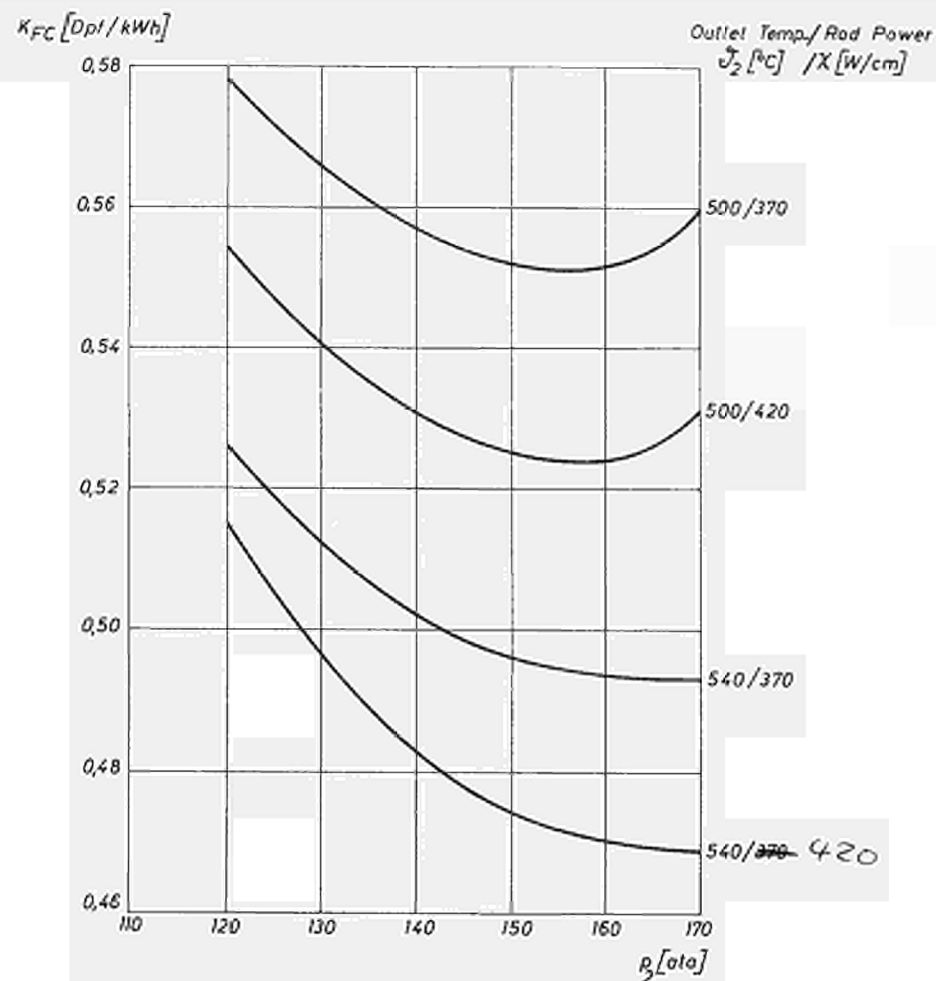


Fig.10 Fuel Cycle Costs vs System Pressure with T_2 and X as Parameters

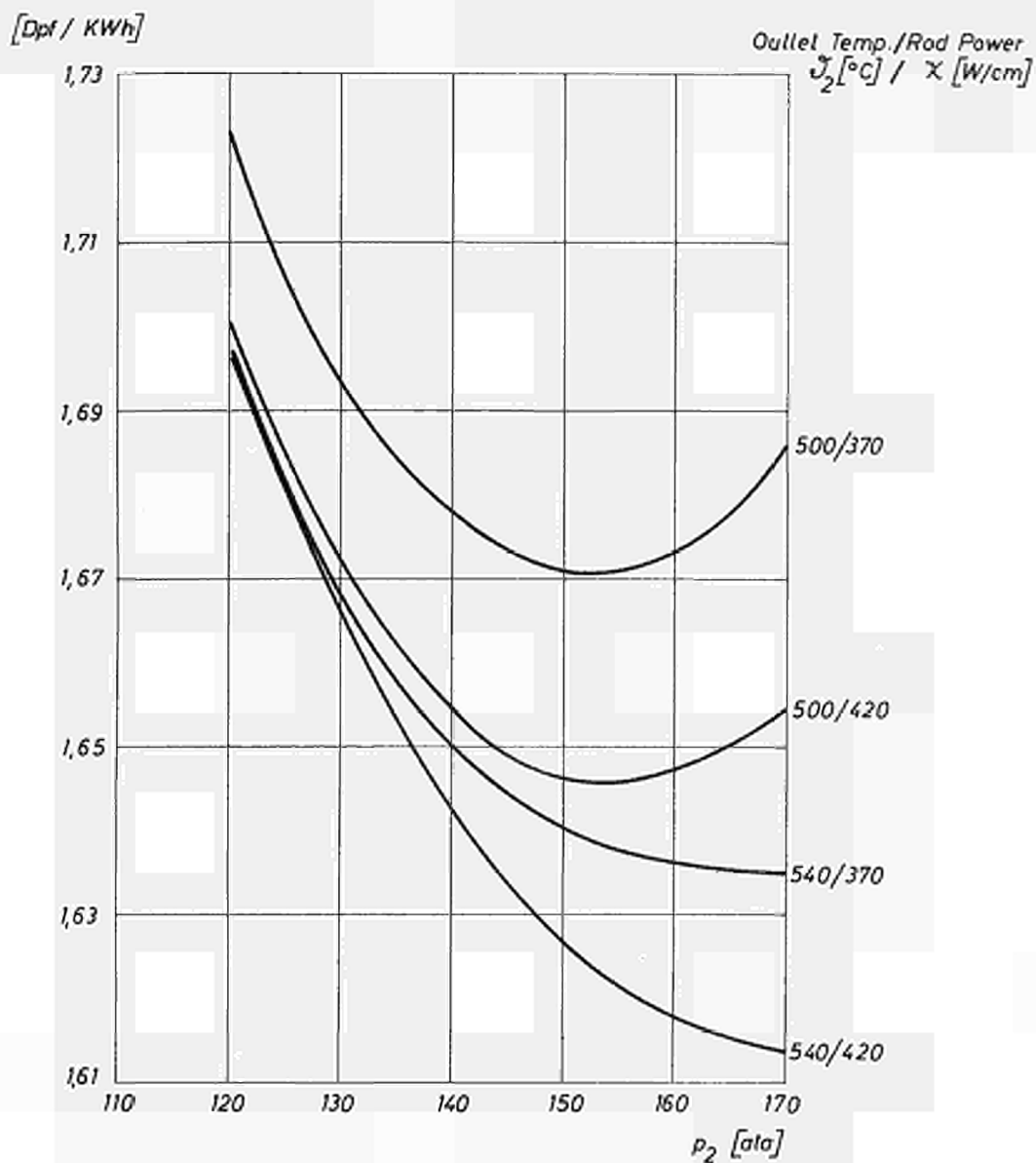


Fig.11 Power Generating Costs vs System Pressure with T_2 and χ as Parameters

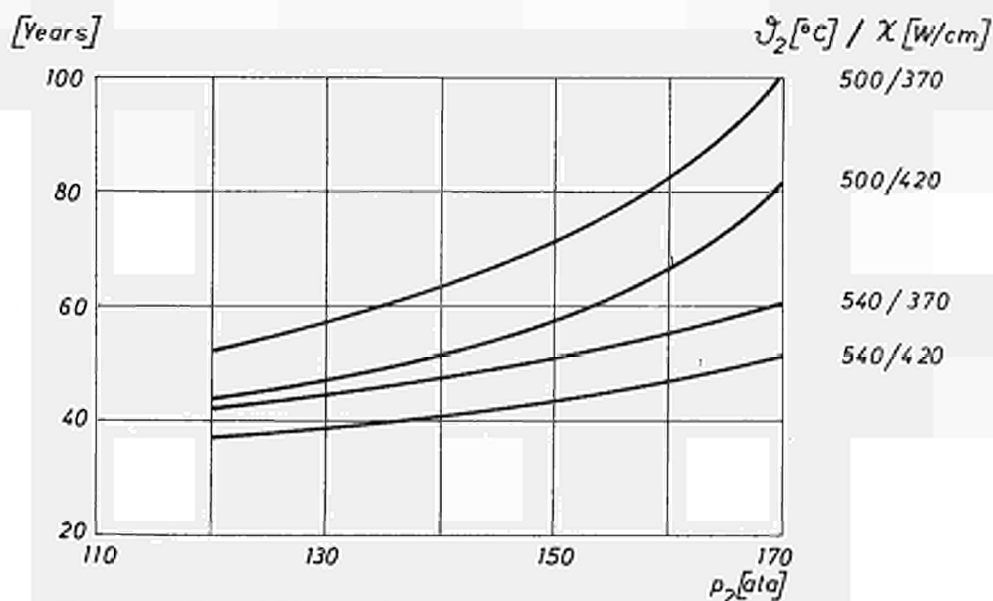


Fig.12 Doubling Time vs System Pressure with T_2 and χ as Parameters

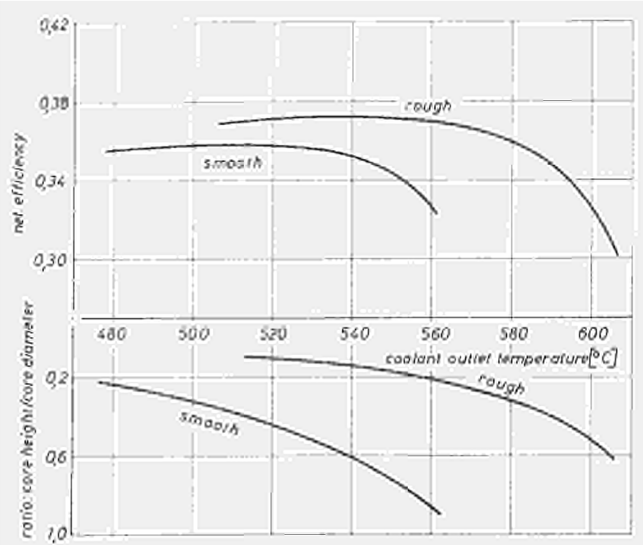


Fig.13 Influence of Artificial Surface Roughening

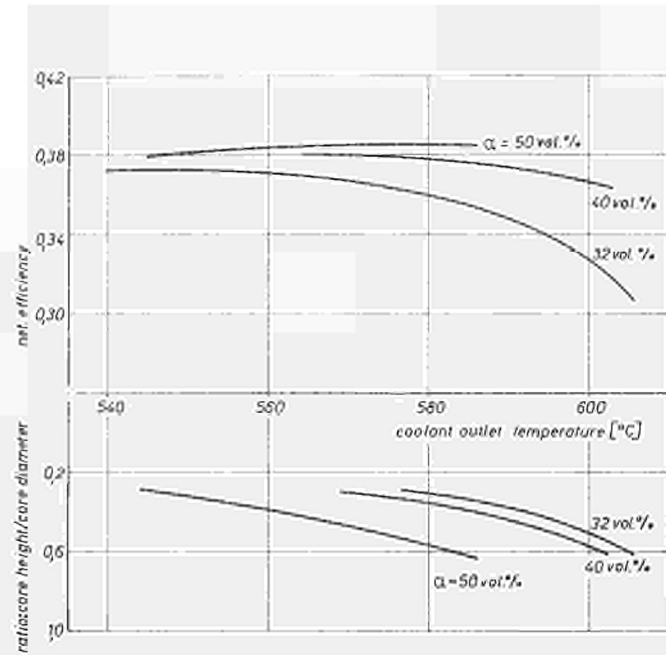


Fig.14 Influence of Coolant Volume Fraction

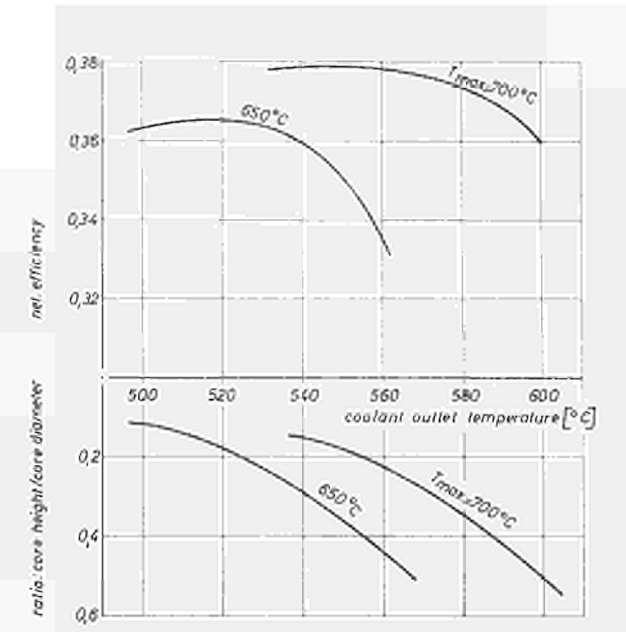
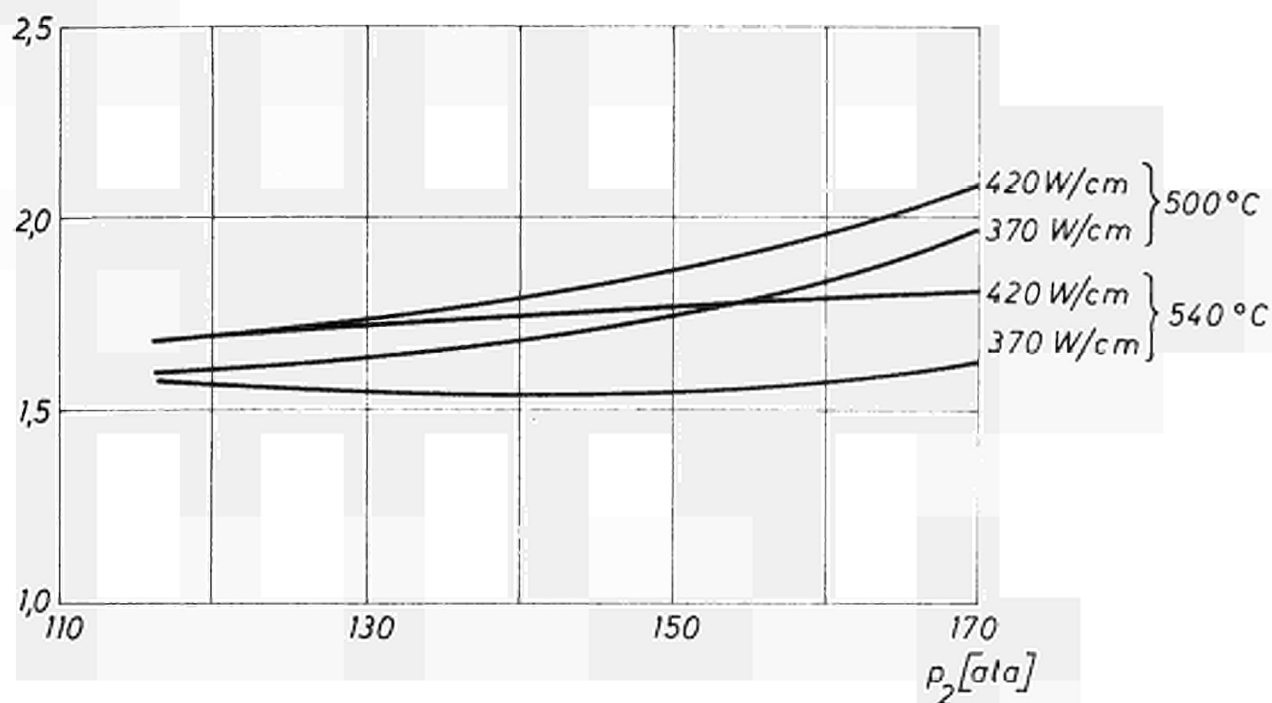


Fig.15 Influence of Can Temperature

$$-\frac{\Delta k}{\Delta P/P} [\%]$$



$$\frac{\alpha_g}{\alpha_{ggr}}$$

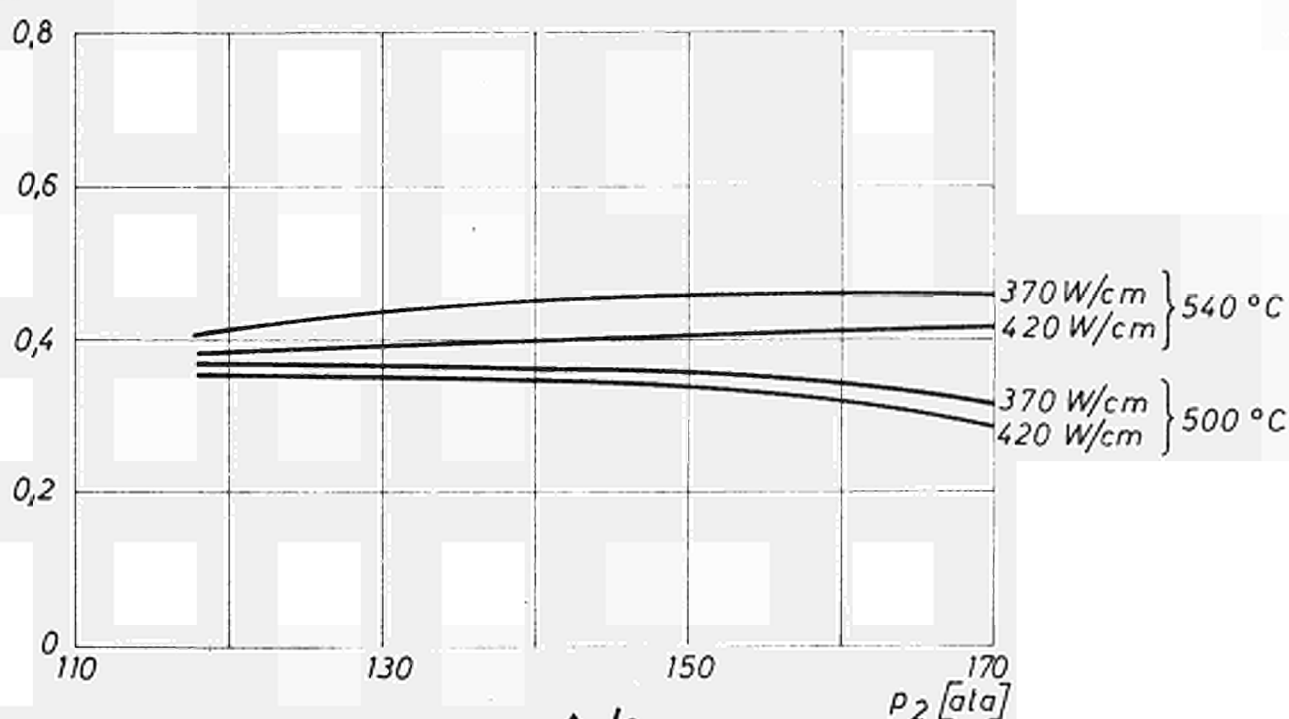


Fig. 16 Power coefficient $\frac{\Delta k}{\Delta P/P}$ and relative distance from the stability boundary α_g/α_{ggr}



CDNA03680ENC